

# Position-Adaptive UAV Radar for Urban Environments

Atindra K. Mitra  
United States Air Force Research Laboratory  
E-mail: atindra.mitra@wpafb.af.mil

**Abstract**—A bistatic radar concept is presented where a low-altitude UAV (Unmanned Aerial Vehicle) “position-adaptively” converges to line-of-sight (LOS) locations for objects that are embedded between buildings. The concept is developed by deriving approximate electromagnetic signal models based on the uniform theory of diffraction (UTD). In addition, a new signature exploitation technique is formulated that allows for the estimation of target parameters in cases when neither the transmitting nor the receiving platform is in LOS with an embedded target or object. This technique is denoted as “exploitation of leakage signals via path trajectory diversity” (E-LS-PTD). Additional areas for further research are cited.

## I. INTRODUCTION

In this paper, a bistatic/multistatic radar system concept is presented for purposes of interrogating difficult and obscured targets via the application of low-altitude “smart” or “robotic-type” UAV platforms. One of the major developments within this concept is the formulation of a UAV system concept that implements self-adaptive positional adjustments based on sensed properties of the propagation channel (i.e. phase discontinuities). In [1] [2], this concept was demonstrated via electromagnetic signal calculations for a tunnel. In this notional tunnel scenario, a small low-altitude UAV was shown to converge to the vicinity of the “throat” of the tunnel in order to interrogate the inside of the tunnel for objects of interest. This concept is further developed for a notional urban environment via analysis of the sample scene in figure 1.

Here, the high-altitude radiating platform is denoted as the HUAV and the low-altitude “position-adaptive” platform is denoted as the LUAV. In section 2, approximate electromagnetic signal models for the sample scenario of figure 1 are derived to define a real-time on-board parameter computation for the LUAV denoted as “signal differential path length”. Computation of the “signal differential path length” allows the LUAV to position-adaptively converge to a location between two buildings. In section 3, the electromagnetic models from section 2 are applied again to develop a new signal exploitation technique denoted as “exploitation of leakage signals via path trajectory diversity” (E-LS-PTD). Section 4 includes a discussion on generalizing the techniques that are developed in sections 2 and 3 for indoor applications as well as other important applications. As a simplifying assumption, all of the analysis is performed in a two-dimensional projection plane as illustrated in figure 2.

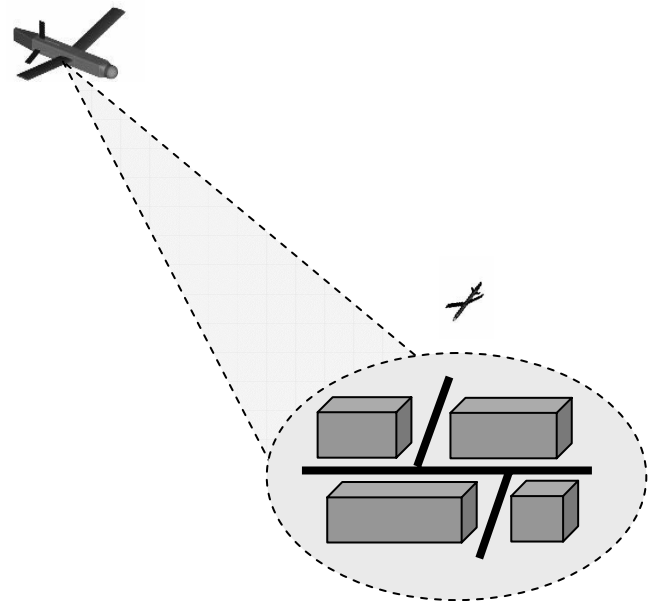


Fig. 1. Sample Urban Scenario for Demonstration of “Position-Adaptive” UAV Concept.

## Position-Adaptive LUAV Converges To “Throat” Of Obscured Channel

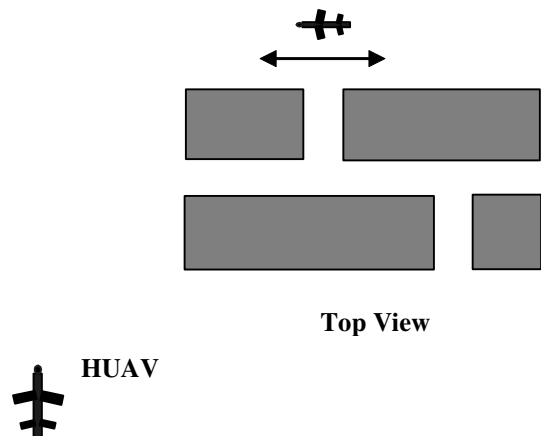


Fig. 2. Two-dimensional “ground plane” projection of figure 1 for purposes of developing analytical signal models.

# Report Documentation Page

*Form Approved*  
*OMB No. 0704-0188*

Public reporting burden for the collection of information is estimated to average 1 hour per response, including the time for reviewing instructions, searching existing data sources, gathering and maintaining the data needed, and completing and reviewing the collection of information. Send comments regarding this burden estimate or any other aspect of this collection of information, including suggestions for reducing this burden, to Washington Headquarters Services, Directorate for Information Operations and Reports, 1215 Jefferson Davis Highway, Suite 1204, Arlington VA 22202-4302. Respondents should be aware that notwithstanding any other provision of law, no person shall be subject to a penalty for failing to comply with a collection of information if it does not display a currently valid OMB control number.

1. REPORT DATE <b>14 APR 2005</b>	2. REPORT TYPE <b>N/A</b>	3. DATES COVERED <b>-</b>	
4. TITLE AND SUBTITLE <b>Position-Adaptive UAV Radar for Urban Environments</b>		5a. CONTRACT NUMBER	
		5b. GRANT NUMBER	
		5c. PROGRAM ELEMENT NUMBER	
6. AUTHOR(S)		5d. PROJECT NUMBER	
		5e. TASK NUMBER	
		5f. WORK UNIT NUMBER	
7. PERFORMING ORGANIZATION NAME(S) AND ADDRESS(ES) <b>United States Air Force Research Laboratory</b>		8. PERFORMING ORGANIZATION REPORT NUMBER	
9. SPONSORING/MONITORING AGENCY NAME(S) AND ADDRESS(ES)		10. SPONSOR/MONITOR'S ACRONYM(S)	
		11. SPONSOR/MONITOR'S REPORT NUMBER(S)	
12. DISTRIBUTION/AVAILABILITY STATEMENT <b>Approved for public release, distribution unlimited</b>			
13. SUPPLEMENTARY NOTES <b>See also ADM001798, Proceedings of the International Conference on Radar (RADAR 2003) Held in Adelaide, Australia on 3-5 September 2003.</b>			
14. ABSTRACT			
15. SUBJECT TERMS			
16. SECURITY CLASSIFICATION OF:			17. LIMITATION OF ABSTRACT
a. REPORT <b>unclassified</b>	b. ABSTRACT <b>unclassified</b>	c. THIS PAGE <b>unclassified</b>	<b>UU</b>
			18. NUMBER OF PAGES <b>6</b>
			19a. NAME OF RESPONSIBLE PERSON

## II. POSITION-ADAPTIVE UAV

For purposes of analyzing basic electromagnetic trends in signals that propagate in an urban environment such as in figure 2, approximate electromagnetic signal models can be derived via application of the uniform theory of diffraction (UTD) [3]. The UTD expression for the electric field at the LUAUV can be expressed as follows:

$$E_r = E_t A_t \sum_{s=1}^S \left( \prod_{m_s}^{M_s} A_R \bar{R} \right) \left( \prod_{n_s}^{N_s} A_D \bar{D} \right) \exp(-jk d_s) \quad (1)$$

where

$E_r$  is the received electric field

$E_t$  is the transmitted electric field

$S$  is number of signal paths from transmitter to receiver

$\bar{R}$  reflection coefficient at  $M_s$  reflection points  
in  $s$ -th signal path

$\bar{D}$  diffraction coefficient at  $N_s$  diffraction points  
in  $s$ -th signal path

$A_t$  spatial attenuation factor from transmitter  
to first reflection point

$A_R$  spatial attenuation factor for reflection points

$A_D$  spatial attenuation factor for diffraction points

$d_s$  length of  $s$ -th signal path

The geometry for this analysis is illustrated in figure 3. This figure illustrates one of the two ray paths that are considered for purposes of deriving approximate signal models. These two ray paths correspond to multiple reflections from the building walls and single diffractions from one of the two building edges formed at the radiating aperture along the signal path shown in figure 3. In this figure, the transmitter coordinates for the HUAUV are denoted as  $(x_t, y_t)$  and the receiver coordinates on the LUAUV are denoted as  $(x_r, y_r)$ . Expressions for the electric field at the LUAUV can be derived by setting  $S=2$ ,  $N_s=1$  in eqn. 1 and evaluating the canonical product terms by splitting the ray paths into segments. For example, for the street segments labeled L1 and L2 in figure 3,

$$d_1 = d_{t1} + dL1_1 + dL12_1 + dL2_1 + d_{r1} \quad (2)$$

Here, the subscript 1 denotes the ray path traced by diffraction from the left building edge in figure 3. The analysis for diffraction from the right building edge is analogous and the equations can be denoted with the subscript 2. The following equations for the multiple ray segments are developed from a straightforward geometrical analysis. This approach is used to develop the computations in the next section.

$$d_{t1} = \frac{y_{t1} + \frac{W}{2}}{\sin(\theta_{t1})} \quad (3)$$

$$\Delta_{L1} = \frac{W}{\cot(\phi_1)}, \quad \Delta_{L2} = \frac{W}{\tan(\phi_1)} \quad (4)$$

$$\Delta_{R1} = \frac{W}{\cos(\phi_1)}, \quad \Delta_{R2} = \frac{W}{\sin(\phi_1)} \quad (5)$$

$$M_{L1} = \frac{L1}{\Delta_{L1}}, \quad M_{L2} = \frac{L2}{\Delta_{L2}} \quad (6)$$

$$dL1_1 = M_{L1} \Delta_{R1} = \frac{L1}{\sin(\phi_1)} \quad (7)$$

$$dL1_2 = M_{L2} \Delta_{R2} = \frac{L2}{\cos(\phi_1)} \quad (8)$$

$$dL12_1 = \Delta_{R1} - \Delta_{R2} \quad (9)$$

$$d_{r1} = \sqrt{\left( y_{r1} - L2 - \frac{W}{2} \right)^2 + \left( x_{r1} + \frac{W}{2} \right)^2} \quad (10)$$

These expressions can be applied to eqn. 1 to obtain compact expressions for the canonical product terms. For example, the canonical product terms for the building reflectivity and attenuation coefficients can be expressed as follows:

$$\left( \prod_{m_s}^{M_s} A_R \bar{R} \right) = \left( \frac{\bar{R}}{\Delta_{R1}} \right)^{M_{L1}} \left( \frac{\bar{R}}{\Delta_{R2}} \right)^{M_{L2}} \quad (11)$$

For analytical purposes, the building edges can be approximated as a perfectly conducting "wedge" and the diffraction coefficient [3] in eqn. 12 can be expressed as follows:

$$\bar{D}_1 = \frac{\exp\left(-j\frac{\pi}{4}\right) \frac{1}{n} \sin\left(\frac{\pi}{n}\right)}{\sqrt{2\pi k}} \bullet P(\phi, \phi') \quad (12)$$

where

$$P(\phi, \phi') = \left[ \frac{1}{\cos\left(\frac{\pi}{n}\right) - \cos\left(\frac{\phi' - \phi}{n}\right)} - \frac{1}{\cos\left(\frac{\pi}{n}\right) - \cos\left(\frac{\phi' + \phi}{n}\right)} \right]$$

$n\pi = \frac{3\pi}{2}$  defines the exterior angle for the building corners,

$$\phi_1 = \frac{\pi}{2} - \theta_{t1} , \quad \phi'_1 = \frac{\pi}{2} + \theta_{r1} ,$$

and  $\theta_{r1} = \frac{\pi}{2} - \text{atan} \left( \frac{y_r - L_2 - \frac{W}{2}}{x_r - \frac{W}{2}} \right)$ .

For this application, one of the predominant characteristics of the signal model of eqn. 12 is the phase term. The “signal path length” for this phase term is expressed by eqn. 2 for ray path 1 (e.g. diffraction from the left building edge). The concept of, as defined in [1] [2], can be defined for this urban application by considering a notional HUAV platform that traverses a trajectory at moderate velocity and with a “phase motion compensation” with respect to a given point within the HUAV trajectory. Under these conditions, and combined with the observation that the HUAV may be located at a relatively far standoff range (e.g. the angular coverage rate of the HUAV is slow), the first four terms of eqn. 2 are approximately equal for any two “phase motion compensated” points on the somewhat localized HUAV trajectory. If these somewhat localized points on the HUAV trajectory correspond to E-field phase measurements on the LUAV, the phase difference between successive measurements is proportional to a quantity denoted as “signal differential path length”. Under the conditions that are stated in the previous paragraph, the “signal differential path length” is proportional to the fifth

term in eqn. 2 and is expressed in eqn. 10 for ray path 1. Under this two-ray-path signal model, the “signal differential path length” for ray path two is proportional to

$$d_{r2} = \sqrt{\left( y_{r2} - L_2 - \frac{W}{2} \right)^2 + \left( x_{r2} - \frac{W}{2} \right)^2} \quad (13)$$

Under these given conditions, if the LUAV loiters back and forth in front of the “radiating aperture” between the two buildings of interest with a given  $y_{r1} \approx y_{r2}$ , the average “signal differential path length” between the two ray paths can be expressed as follows:

$$d_{AVE} = \sqrt{\left( y_r - L_2 - \frac{W}{2} \right)^2 + (x_r)^2} \quad (14)$$

From inspection, eqn. 14 is minimized when  $x_r = 0$ . Therefore, with this “position-adaptive” system, a LUAV can loiter back and forth and then converge to a location between two buildings of interest by performing real-time onboard calculations of “signal differential path length”. Alternatively, a LUAV can also measure the phase discontinuities generated by “interference patterns” between the two ray paths in the signal model of eqn. 1.

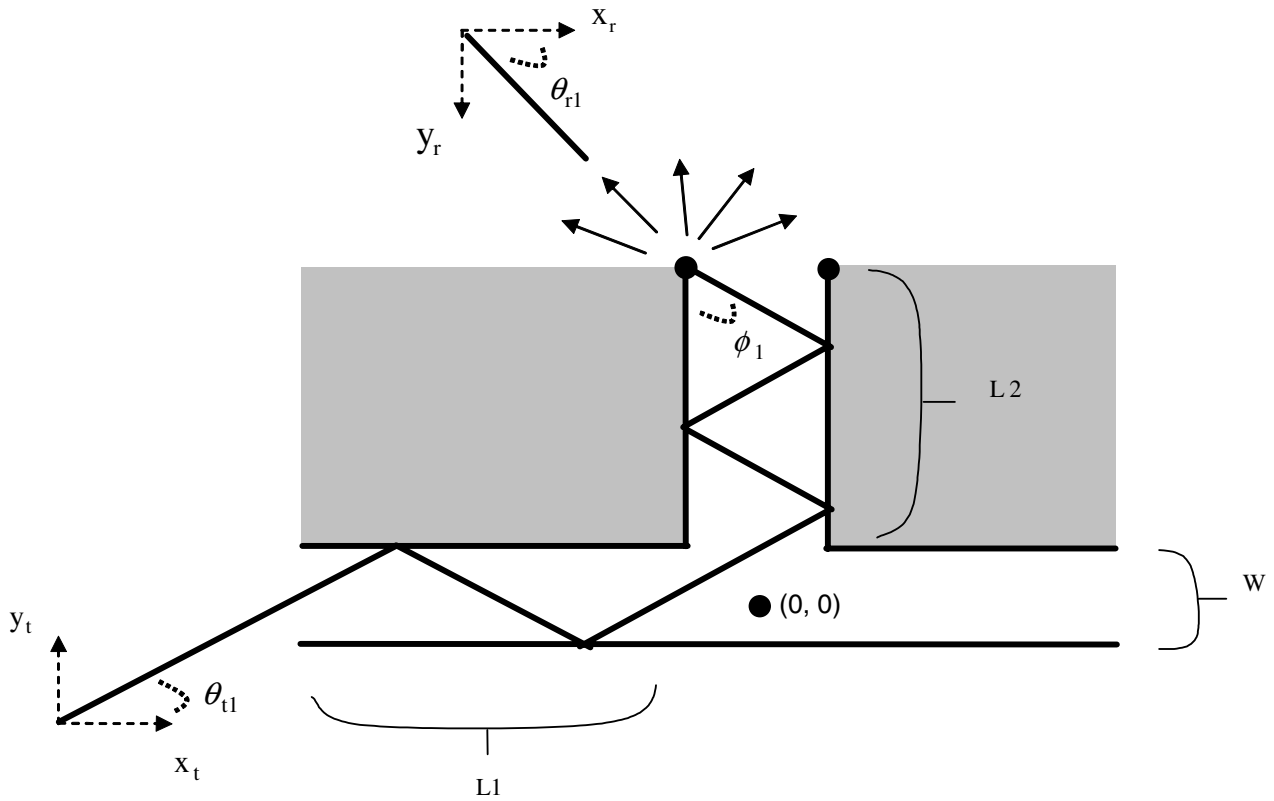


Fig. 3. Geometry for Sample Urban Scenario of Fig. 2

For example, analysis of the resultant phase term in eqn. 1 for  $S=2$  yields a sharp phase discontinuity at a receiver location that is centered between the two buildings and more gradual phase discontinuities for receiver locations that correspond to the edges of the two buildings. Analysis of these overall trends and discontinuities in these phase characteristics can enable a LUAV to “position-adaptively” converge a location between two buildings. Then, the LUAV can interrogate the region between the buildings for embedded objects of interest.

### III. LEAKAGE SIGNAL EXPLOITATION

Under the “position-adaptive” systems concept in [1] [2], after the LUAV converges to the vicinity of an embedded channel, the LUAV enters a close-range interrogation mode with an on-board low-power active radar or ladar sensor. In this section, a bistatic approach to interrogating the embedded channel is described that allows the LUAV to remain passive. The two-dimensional geometry for analysis and development of this approach is shown in figure 4. A embedded target is shown, coded in black, as a rectangular box. This target is not within the line-of-sight of either the LUAV or the HUAV.

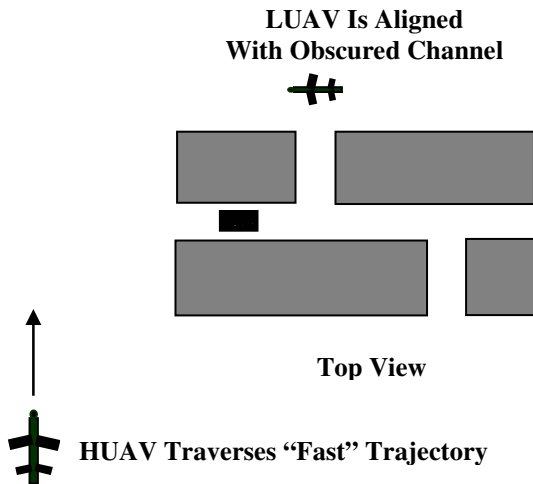


Fig. 4. Two-dimensional view of signature exploitation geometry

Under this approach, the system enters a second mode after the LUAV has already “position-adaptively” converged to a location between buildings. In this second mode, the LUAV hovers in the vicinity of the channel opening and the HUAV flies a “fast trajectory” in order to generate a signal signature from the embedded target as a function of HUAV transmitter angle. This technique is denoted as “exploitation of leakage signals via path trajectory diversity” (E-LS-PTD). Figure 5 illustrates two geometries that fall within the trajectory of the HUAV. An analysis of this concept is performed with the electromagnetic signal models developed in section 2. For example, the “backscatter” condition in Figure 5a is predicted from the following logical operation and application of eqn. 6:

$$\begin{aligned} \text{IF } \text{frac}\left(M_{L1_1} = \frac{L1_1}{\Delta_{L1}}\right) > .25 \\ \text{AND } \text{frac}\left(M_{L1_1} = \frac{L1_1}{\Delta_{L1}}\right) < .75 \quad (15) \\ E_r = 0 \end{aligned}$$

Signal models for the “forward-scatter” condition of figure 5b are computed by coding eqns. 1 – 10 for simulating two ray paths. Street L1 is split into sections L1\_1, LX, and L1\_2 and the formulas are applied to each of these three sections separately. Using this approach, Figure 6 is a plot of the electric field computation at a receiver as a function of transmitter beam angle (from 30 to 60 degrees) for a notional building reflectivity of 1 and a notional target reflectivity of .5. Some of the additional notional systems and geometrical parameters used for this computation are as follows:

Xmitter Ave. Power: 10 KW  
Signal Frequency: 10GHz  
Xmitter Antenna Gain: 30dB  
Xmitter Range in x-dir: 5Km  
Receiver Range in y-dir: 500m

L1=100m, L2=100m, W=20m  
LX=25m, WX=10m, L1\_2=37.7m

Observation of this plot indicates that the duration of the “signal valley” is proportional to WX and the duration of the signal between the neighboring “signal valleys” is proportional to LX. The ratio of the duration of these two signal segments is approximately equal to the ratio of LX and WX. This notional set of computations is intended to show that signals from the E-LS-PTD technique can be processed to estimate parameters for embedded objects of interest.

### IV. SUMMARY

A “position-adaptive” bistatic radar system concept for low-altitude near-range sensing applications was presented. This system concept is developed for applications where a target or object of interest is embedded in an obscured channel. The focus of this particular investigation was an outdoor urban environment. Future investigations, simulations, and data collections are planned for further development and maturation of this concept in an outdoor urban environment as well as for interrogation of indoor urban environments, tunnels, embedded cavities, and other challenging clutter environments.

For example, for monitoring indoor environments three spatial degrees of freedom (including elevation) can be used instead of two. With this approach, the LUAV can be positioned along the line-of-sight of, for example, a window of a particular floor to investigate the possible characterization of objects and personnel within buildings. In order to analyze these types of environments, the approximate signal models that were developed for this investigation will can be modified to accommodate

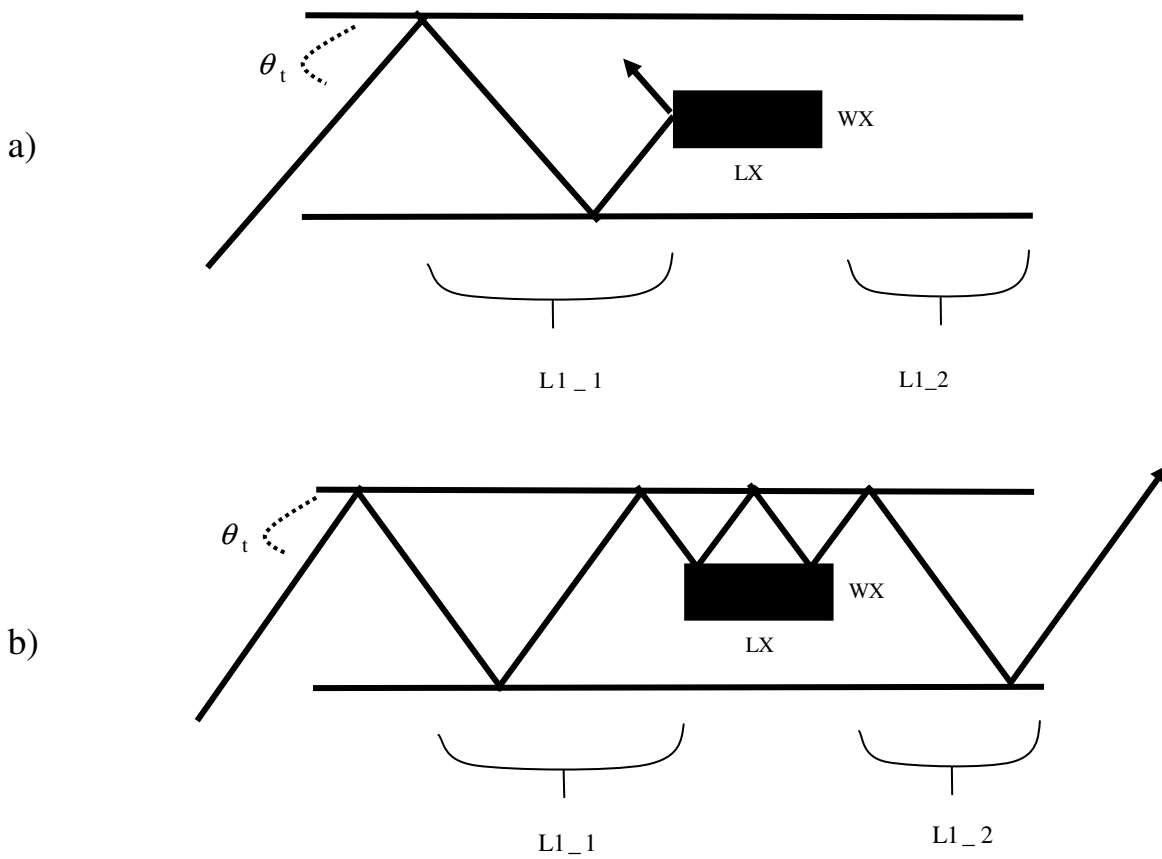


Fig. 5. Two predominant signal paths with embedded object as function of transmitter trajectory and beam angle.

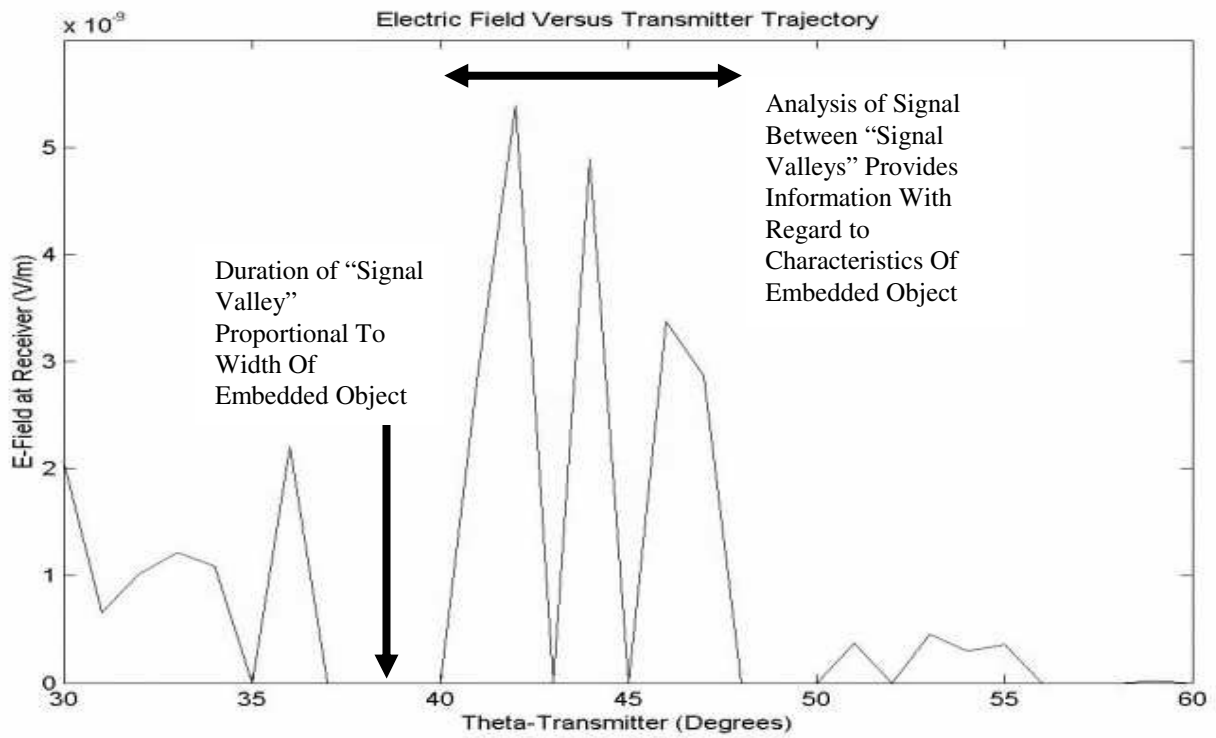


Fig. 6. Electric field signal as a result of computations with the signal models from section 2. Signal can be analyzed to extract characteristics of embedded object

lower-frequency signals with transmission coefficients that penetrate or “leak” through the outer structures of buildings.

In addition, there are a number of options for generalizing the E-LS-PTD technique to estimate target and object characteristics in three dimensions as well as to estimate more complex characteristics for moving and stationary targets. These options include applying additional spatial degrees of “position adaptation” as in the indoor case as well as via implementing additional “smart” flights paths for the LUAV after the LUAV converges to “look down the throat” of a obscuration channel. In addition, strategies for employing multiple UAV’s are under consideration. Technology challenges in this new area include further characterization of signal strengths as a function of environmental material properties and relative distance of separation between the platforms. There is also potential for the development of advanced signal processing techniques for purposes of extracting additional information for a target or object of interest. Future plans include the implementation of a series of high-fidelity simulations and measurements in an effort to further develop this concept for a variety of challenging environments

#### V. REFERENCES

- [1] Atindra Mitra , “Multi-Level UAV Exploitation for Environments with Difficult and Obscured Targets,” Proceedings of the Eight Annual Joint Aerospace Weapon Systems Support, Sensors, and Simulation Symposium and Exhibition, 24 July 2002
- [2] Atindra Mitra, Pending Patent entitled “Multi-Static UAV Radar System for Mode-Adaptive Propagation Channels with Obscured Targets,” Air Force Invention Number AFD 609
- [3] Henry L. Bertoni, *Radio Propagation for Modern Wireless Systems*, Prentice-Hall, 200